Available online at www.derpharmachemica.com

ISSN 0975-413X
CODEN (USA): PCHHAX

Der Pharma Chemica, 2016, 8(14):1-9
(http://derpharmachemica.com/archive.html)

A DFT study of the inhibition of FMS-like tyrosine kinase 3 and the antiproliferative activity against MV4-11 cells by *N*-(5-(*tert*-butyl)isoxazol-3-yl)-*N'*-phenylurea analogs

Juan S. Gómez-Jeria* and Richard Salazar

Quantum Pharmacology Unit, Department of Chemistry, Faculty of Sciences, University of Chile, Las Palmeras 3425, Santiago 7800003, Chile

---

ABSTRACT

We performed an analysis of the relationships between the electronic structure of N-(5-(tert-butyl)isoxazol-3-yl)-N'-phenylurea analogs and two activities: the inhibition of FMS-like tyrosine kinase 3 and the antiproliferative action against MV4-11 cells. The electronic structure of all molecules was calculated within the Density Functional Theory at the B3LYP/6-31g(d,p) level with full geometry optimization. For each biological activity linear multiple regression analysis techniques were employed to find the best relationship between the biological activities and local atomic reactivity indices belonging to a common skeleton. We found statistically significant results for both activities. The corresponding partial pharmacophores are presented. Both biological processes seem to be orbital- and geometrical-controlled.

Keywords: Acute myeloid leukemia, FMS-like tyrosine kinase 3, FLT3, QSAR, DFT, MV4-11 cells.

INTRODUCTION

Acute myeloid leukemia (AML) is a malignant proliferation of hematopoietic progenitor cells of the myeloid lineage inside the bone marrow. These poorly differentiated precursor cells stop to function normally and interrupt the regular hematopoiesis causing bleeding, infection and multi-organ dysfunction. Today, the diagnosis and classification of a patient with AML incorporates both chromosomal analysis and the presence or absence of somatically acquired gene mutations. Mutations in the FMS-like (FLT3) gene represent one of the most frequently encountered class of AML mutations and are particularly common in adult AML with an overall incidence of about 20% to 30%. The FLT3 gene codes for a transmembrane receptor/signaling protein (FLT3) of the tyrosine kinase cluster. The binding of the FLT3 ligand to the FLT3 receptor in the end leads to production of proteins that produce cell growth and inhibit cell death through apoptosis [1]. Considering the prevalence and propensity for poor outcome in AML patients carrying FLT3 mutations, a continued effort is ongoing to develop inhibitors of FLT3 [2-7]. A diversity of compounds has gone into clinical trials and various have met with success (Sunitinib, Sorafenib, Midostaurin and Lestaurtinib for example).

Here we present the results of a study relating the electronic structure of a group of recently published *N*-(5-(tert-butyl)isoxazol-3-yl)-*N'*-phenylurea analogs and two biological activities: their antiproliferative activity against MV4-11 cells (cell line established from a 10-year-old boy with acute monocytic leukemia) and the inhibition of FMS-like tyrosine kinase 3 [4].

Methods, models and calculations

As the method employed (The Klopman-Peradejordi-Gómez method, KPG) here has been presented [8-14], discussed and applied in many previous papers [15-30] (and references therein), we present here only a short summary. The biological activity is related by a linear equation to several local reactivity indices of the atoms composing the common skeleton, the molecular mass and the orientational parameter of the substituents [12]. The local atomic reactivity indices are the net charge, the total atomic electrophilic and nucleophilic superdelocalizabilities, the Fukui index of a chosen set of vacant and occupied MOs, the electrophilic superdelocalizability of a chosen set of occupied MOs, the nucleophilic superdelocalizability of a chosen set of vacant MOs, the local atomic electronic chemical potential (a measure of the tendency of an atom to gain or lose electrons), the local atomic hardness (the resistance of an atom to exchange electrons with the environment), the local atomic softness, the local electrophilic index of atom (associated with the electrophilic power of an atom and includes the tendency of the electrophile atom to receive extra electronic charge together with its resistance to exchange charge with the medium) and the maximal amount of electronic charge that an electrophile may accept [31, 32]. The fundamental importance of this relation is that it contains only terms belonging to the drug molecules. The orientational parameters of the substituent are always positive. They come from a classical analysis of the rotational partition function [11]. To interpret them, let us imagine a group of molecules approaching to a binding site. Their velocities will vary accordingly to their interactions with the surrounding fluid that is in constant circulation. On its hand, the binding sites producing biological effects are structures that by evolutionary processes bind to only very specific endogenous molecules (and also some exogenous agents). This specificity seems to be determined by the molecular electrostatic potential for recognition at medium molecule-site distances and through non-covalent interactions at shorter distances. Circulation carries a molecule close to the binding site. Now, and given that the *milieu* is in constant circulation, only the molecules having the right rotational velocities will be able to spend the proper time close to the binding site, allowing it to recognize and attract them. We have proposed that the orientational parameters are related to this critical time interval.

The selected molecules are a group of *N*-(5-(tert-butyl)isoxazol-3-yl)-*N'*-phenylurea analogs. The biological activities analyzed here are the FLT3 inhibition (expressed as the percentage of inhibition at 100 nM, I) and the *in vitro* antiproliferative activity against MV4-11 cells (expressed as IC_{50}) [4]. The molecules and their biological activities are shown in Fig. 1 and Table 1.

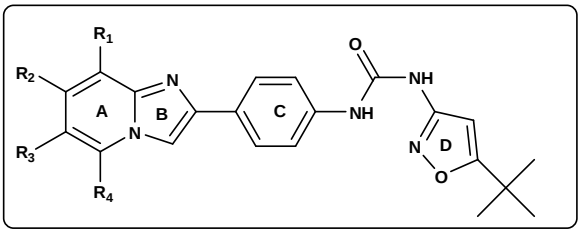

Figure 1. General formula of *N*-(5-(*tert*-butyl)isoxazol-3-yl)-*N'*-phenylurea analogs

The electronic structure of all molecules was calculated within the Density Functional Theory at the B3LYP/6-31g(d,p) level with full geometry optimization. The Gaussian suite of programs was used. [33] All the information required to calculate the numerical values for the local atomic reactivity indices was obtained from the Gaussian results with the D-Cent-QSAR software [34]. All the electron populations smaller than or equal to 0.01 e were considered as zero [31]. The negative electron populations produced by Mulliken Population Analysis were rectified as usual [35]. Orientational parameters were calculated as usual or taken from published Tables [13, 14]. As the resolution of the system of linear equations is not possible for the reason that we have not sufficient molecules, we employed Linear Multiple Regression Analysis (LMRA) techniques to discover the best solution. For each case, a matrix containing the dependent variable (the biological activity of each case) and the local atomic reactivity indices of all atoms of the common skeleton as independent variables was constructed. The Statistica software was employed for LMRA [36].

Table 1. *N*-(5-(*tert*-butyl)isoxazol-3-yl)-*N'*-phenylurea analogs and their biological activities

Mol.	R1	R2	R3	R4	log(IC_{50}) MV4-11	log(I) FLT3
1	H	H	H	H	0.49	1.82
2	F	H	H	H	1.09	1.59
3	Cl	H	H	H	2.55	1.10
4	Me	H	H	H	2.40	1.13
5	CF3	H	H	H	2.95	0.40
6	H	Cl	H	H	0.77	1.65
7	H	Br	H	H	0.98	1.60
8	H	Me	H	H	-0.10	1.84
9	H	-C≡CH	H	H	0.54	1.76
10	H	OMe	H	H	0.45	1.76
11	H	OEt	H	H	1.06	1.65
12	H	-OCH(O)	H	H	1.47	1.44
13	H	H	F	H	1.32	1.50
14	H	H	Cl	H	1.39	1.55
15	H	H	Br	H	1.65	1.45
16	H	H	Me	H	0.61	1.69
17	H	H	-C≡CH	H	0.94	1.60
18	H	H	c-Pr	H	1.20	1.48
19	H	H	H	Cl	1.75	1.45
20	H	H	H	Me	1.31	1.62

We worked within the *common skeleton approximation* affirming that there is a certain collection of atoms, shared by all the molecules analyzed, that accounts for practically all the biological activity. The effect of the substituents consists in changing the electronic structure of the common skeleton and influencing the precise placement of the drug through the orientational parameters. It is hypothesized that different parts or this common skeleton accounts for almost all the interactions leading to the expression of a particular biological activity. The common skeleton is shown in Fig. 2.

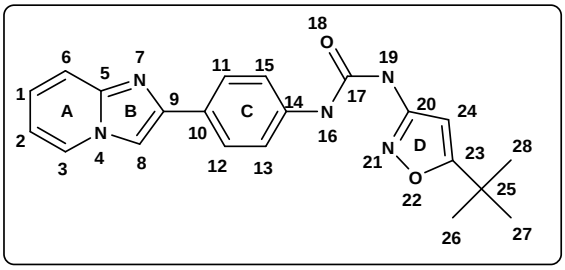

Figure 2. Common skeleton numbering for the linear multiple regression analysis

Results for the percentage of inhibition of FLT3 (I).

The best equation obtained is:

$$\log(I)=1.63-0.004\Phi_{R1}-0.26S_{18}^{N}(LUMO)^{*}+0.03S_{16}^{N}(LUMO)^{*}-0.0008\Phi_{R3}-0.002\Phi_{R4} \quad (1)$$

with n=19, R= 0.99, R^2= 0.97, adj-R^2= 0.96, F(5,13)=96.544 ($p< 0.000001$) and a standard error of estimate of 0.06. Here, Φ_{R1} is the orientational parameter of the R_1 substituent, $S_{18}^{N}(LUMO)^{*}$ is the nucleophilic superdelocalizability of the lowest vacant MO localized on atom 18, $S_{16}^{N}(LUMO)^{*}$ is the nucleophilic superdelocalizability of the lowest vacant MO localized on atom 16, Φ_{R3} is the orientational parameter of the R_3 substituent and Φ_{R4} is the orientational parameter of the Φ_{R4} substituent. Tables 2 and 3 show the beta coefficients, the results of the t-test for significance of coefficients and the matrix of squared correlation coefficients for the variables of Eq. 1. There are no significant internal correlations between independent variables (Table 3). Figure 3 displays the plot of observed *vs.* calculated log(I).

Table 2. Beta coefficients and t-test for significance of coefficients in Eq. 1

	Beta	t(13)	p-level
φ_{R1}	-1.06	-19.60	<0.000001
S^N_{18}(LUMO)*	-0.17	-2.96	<0.01
S^N_{16}(LUMO)*	0.21	4.36	<0.0008
φ_{R3}	-0.19	-4.06	<0.001
φ_{R4}	-0.18	-3.88	<0.002

Table 3. Matrix of squared correlation coefficients for the variables in Eq. 1

	φ_{R1}	S^N_{18}(LUMO)*	S^N_{16}(LUMO)*	φ_{R3}
S^N_{18}(LUMO)*	0.30	1.00		
S^N_{16}(LUMO)*	0.00	0.04	1.00	
φ_{R3}	0.03	0.07	0.00	1.00
φ_{R4}	0.01	0.01	0.04	0.03

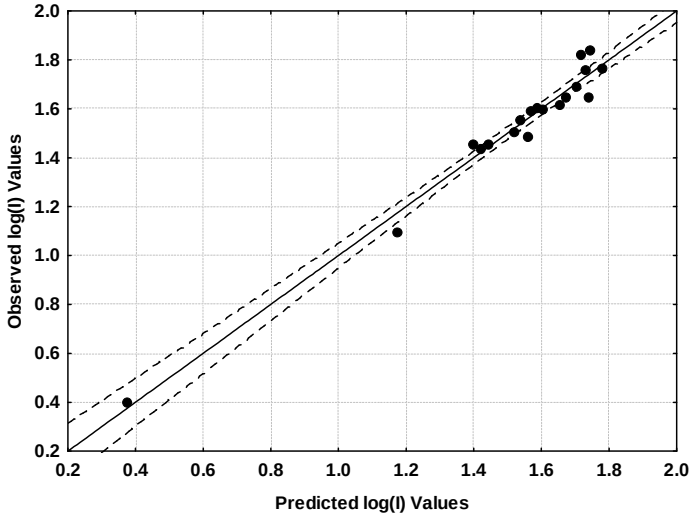

Figure 3. Plot of predicted *vs.* observed log(I) values (Eq. 1). Dashed lines denote the 95% confidence interval

The associated statistical parameters of Eq. 1 indicate that this equation is statistically significant and that the variation of the numerical values of a group of five local atomic reactivity indices of atoms of the common skeleton explains about 96% of the variation of log(I) in this group of molecules. Figure 3, spanning about 1.4 orders of magnitude, shows that there is a good correlation of observed *versus* calculated values and that almost all points are inside the 95% confidence interval.

Results for the inhibition of MV4-11 cells.

The best equation obtained is:

$$\log(IC_{50}) = 1.34 + 0.007\Phi_{R1} - 0.15S^N_{28}(\text{LUMO})^* + 3.00S^N_{18}(\text{LUMO})^* - 1.56F_{13}(\text{LUMO+1})^* - 5.59S^E_8(\text{HOMO-2})^* - 0.18S^N_6(\text{LUMO})^* \quad (2)$$

with n=18, R= 0.98, R^2= 0.95, adj-R^2= 0.93, F(6,11)=37.959 ($p< 0.000001$) and a standard error of estimate of 0.18. Here, Φ_{R1} is the orientational parameter of the R_1 substituent, $S_{28}{}^N$(LUMO)* is the nucleophilic superdelocalizability of the lowest vacant MO localized on atom 28, $S_{18}{}^N$(LUMO)* is the nucleophilic superdelocalizability of the lowest vacant MO localized on atom 18, F_{13}(LUMO+1)* is the Fukui index (electron population) of the second vacant MO localized on atom 13, $S_8{}^E$(HOMO-2)* is the electrophilic superdelocalizability of the third highest occupied MO localized on atom 8 and $S_6{}^N$(LUMO)* is the nucleophilic superdelocalizability of the lowest vacant MO localized on

atom 6. Tables 4 and 5 show the beta coefficients, the results of the t-test for significance of coefficients and the matrix of squared correlation coefficients for the variables of Eq. 2. There are no significant internal correlations between independent variables (Table 5). Figure 4 displays the plot of observed *vs.* calculated log(IC_{50}).

Table 4. Beta coefficients and t-test for significance of coefficients in Eq. 2

	Beta	t(11)	p-level
φ_{R1}	0.99	11.16	<0.000001
S^{N}_{28}(LUMO)*	-0.56	-5.99	<0.00009
S^{N}_{18}(LUMO)*	0.96	8.42	<0.000004
F_{13}(LUMO+1)*	-0.44	-4.50	<0.001
S^{E}_{8}(HOMO-2)*	-0.64	-6.27	<0.00006
S^{N}_{6}(LUMO)*	-0.22	-2.76	<0.02

Table 5. Matrix of squared correlation coefficients for the variables in Eq. 2

	φ_{R1}	S^{N}_{28}(LUMO)*	S^{N}_{18}(LUMO)*	F_{13}(LUMO+1)*	S^{E}_{8}(HOMO-2)*
S^{N}_{28}(LUMO)*	0.03	1.00			
S^{N}_{18}(LUMO)*	0.31	0.01	1.00		
F_{13}(LUMO+1)*	0.02	0.18	0.10	1.00	
S^{E}_{8}(HOMO-2)*	0.20	0.12	0.37	0.04	1.00
S^{N}_{6}(LUMO)*	0.00	0.02	0.10	0.20	0.00

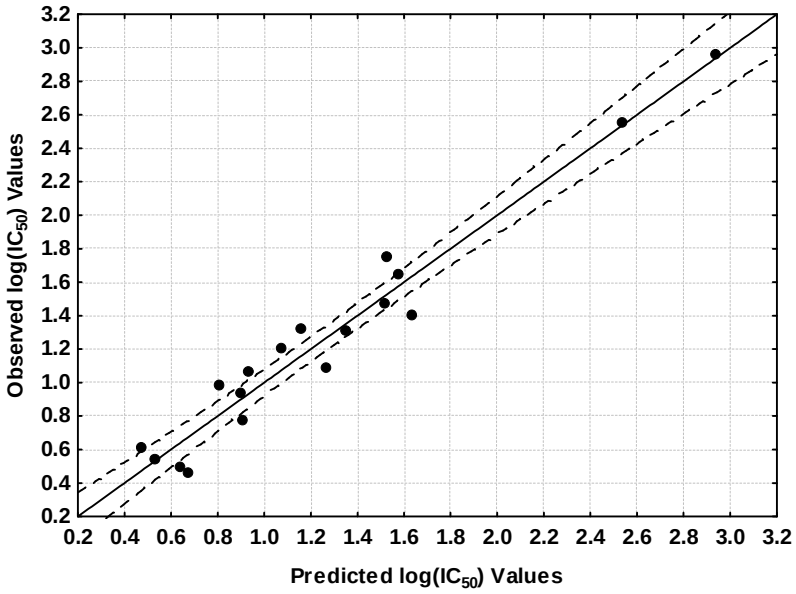

Figure 4. Plot of predicted *vs*. observed log(IC_{50}) values (Eq. 2). Dashed lines denote the 95% confidence interval

The associated statistical parameters of Eq. 2 indicate that this equation is statistically significant and that the variation of the numerical values of a group of six local atomic reactivity indices of atoms of the common skeleton explains about 93% of the variation of log(IC_{50}) in this group of molecules. Figure 4, spanning about 2.5 orders of magnitude, shows that there is a good correlation of observed *versus* calculated values and that almost all points are inside the 95% confidence interval.

Local Molecular Orbitals.

Tables 6 and 7 show the local MO structure of atoms with reactivity indices appearing in Eq. 1 and 2 (see Fig. 2). Nomenclature: Molecule (HOMO) / (HOMO-2)* (HOMO-1)* (HOMO)* - (LUMO)* (LUMO+1)* (LUMO+2)*.

Table 6. Local molecular orbitals of atoms 6, 8 and 13

Mol.	Atom 6 (C)	Atom 8 (C)	Atom 13 (C)
1 (99)	96π98π99π-101π102π103π	95π98π99π-100π101π103π	95π98π99π-100π102π103π
2 (103)	100π102π103π-105π106π107π	99π102π103π-104π105π106π	99π102π103π-104π106π107π
3 (107)	104π106π107π-109π110π111π	103π106π107π-108π109π111π	103π106π107π-108π110π111π
4 (103)	99π100π103π-105π106π107π	100π102π103π-104π105π106π	100π102π103π-104π105π106π
5 (115)	111π114π115π-117π118π119π	113π114π115π-117π119π121π	113π114π115π-116π118π119π
6 (107)	103π106π107π-109π110π111π	103π106π107π-108π109π111π	103π106π107π-108π110π111π
7 (116)	112π115π116π-118π119π120π	112π115π116π-117π118π121π	112π115π116π-117π119π121π
8 (103)	100π102π103π-105π106π107π	99π102π103π-104π105π106π	98π102π103π-104π105π106π
9 (105)	100π101π105π-106π107π108π	98π104π105π-107π109π111π	100π104π105π-106π107π108π
10 (107)	103π106π107π-109π110π112π	101π103π107π-108π109π111π	103π106π107π-108π110π111π
11 (111)	108π110π111π-113π114π116π	105π107π111π-112π113π115π	107π110π111π-112π114π115π
12 (114)	109π110π114π-116π117π118π	110π113π114π-115π116π118π	110π113π114π-115π117π119π
13 (103)	100π102π103π-105π106π107π	99π102π103π-105π107π108π	99π102π103π-104π106π107π
14 (107)	104π106π107π-109π110π111π	103π106π107π-109π111π112π	103π106π107π-108π110π111π
15 (116)	113π115π116π-118π119π121π	112π115π116π-117π118π120π	112π115π116π-117π119π121π
16 (103)	100π102π103π-105π106π107π	99π102π103π-104π105π106π	100π102π103π-104π106π107π
17 (105)	103π104π105π-106π107π108π	102π104π105π-106π107π108π	102π104π105π-106π107π108π
18 (110)	107π109π110π-112π113π114π	106π109π110π-111π112π114π	107π109π110π-111π113π114π
19 (107)	103π106π107π-109π110π111π	103π106π107π-108π109π110π	103π106π107π-108π110π111π
20 (103)	99π100π103π-105π107π108π	99π102π103π-104π105π106π	100π102π103π-104π105π106π

Table 7. Local molecular orbitals of atoms 16, 18 and 28

Mol.	Atom 16 (N)	Atom 18 (O)	Atom 28 (C)
1 (99)	96π98π99π-100π103π105π	96π97π99π-100π101π102π	88σ89σ91σ-106σ117σ120σ
2 (103)	100π102π103π-104π107π108π	100π101π103π-104π105π106π	91σ92σ95σ-110σ120σ121σ
3 (107)	104π106π107π-111π112π114π	104π105π107π-108π109π110π	95σ104σ105σ-111σ114σ121σ
4 (103)	100π102π103π-104π107π109π	100π101π103π-104π105π106π	91σ92σ95σ-110σ122σ125σ
5 (115)	113π114π115π-119π120π121π	113π114π115π-117π118π119π	107σ112σ113σ-120σ121σ122σ
6 (107)	104π106π107π-108π111π113π	104π105π107π-108π109π110π	99σ104σ105σ-111σ113σ114σ
7 (116)	113π115π116π-121π122π123π	113π114π116π-117π118π119π	104σ113σ114σ-121σ123σ130σ
8 (103)	100π102π103π-104π107π109π	101π102π103π-104π105π106π	95σ100σ101σ-107σ109σ110σ
9 (105)	102π104π105π-109π110π111π	103π104π105π-107π108π109π	92σ93σ95σ-113σ124σ125σ
10 (107)	104π106π107π-108π111π113π	105π106π107π-108π109π110π	96σ104σ105σ-111σ113σ122σ
11 (111)	108π110π111π-112π115π117π	109π110π111π-112π113π114π	100108109-115117126
12 (114)	111π113π114π-119π121π123π	112π113π114π-115π116π117π	105σ111σ112σ-119σ121σ122σ
13 (103)	100π102π103π-107π109π112π	100π101π103π-104π105π106π	92σ93σ95σ-110σ121σ125σ
14 (107)	104π106π107π-111π113π114π	104π105π107π-108π109π110π	97σ104σ105σ-111σ114σ120σ
15 (116)	113π115π116π-121π122π123π	113π114π116π-117π118π119π	105σ113σ114σ-121σ123σ129σ
16 (103)	101π102π103π-104π107π109π	100π101π103π-104π105π106π	91σ92σ95σ-110σ122σ125σ
17 (105)	103π104π105π-106π110π111π	101π103π105π-106π108π110π	92π93σ95σ-113σ125σ128σ
18 (110)	108π109π110π-111π114π116π	106π108π110π-111π112π113π	98σ107σ108σ-114σ116σ125σ
19 (107)	104π106π107π-108π112π113π	104π105π107π-108π109π110π	97σ104σ105σ-112σ114σ121σ
20 (103)	100π102π103π-104π107π109π	101π102π103π-104π105π106π	91σ92σ95σ-110σ122σ125σ

DISCUSSION

Discussion of the percentage of inhibition of FLT3 (I).

The beta values (Table 2) indicate that the importance of variables is φ_{R1}>>> S^N_{16}(LUMO)* > φ_{R3} > φ_{R4} > S^N_{18}(LUMO)*. Noting that 2.0 is the greatest value for log(I) and that a good percentage of inhibition is associated with a large value for log(I), the numerical values for the three orientational parameters appearing in Eq. 1 must be small. We can see from Table 1 that the optimal situation is $R_1 = R_3 = R_4 = H$. Nevertheless it seems that the H atom (OP =1.18) can be replaced by fluorine (OP = 40.0) with only a relatively small change in activity. Atom 18 is the carbonyl oxygen in the chain linking rings C and D (Fig. 2). If the value of S^N_{18}(LUMO)* is positive, a small numerical value is associated with high percentage of inhibition. A small numerical value is obtained by rising the $(LUMO)_{18}$* eigenvalue or by finding a substitution suppressing the localization of the molecular LUMO in atom 18 (in this case $(LUMO)_{18}$* should correspond to an empty vacant MO lying energetically far from the molecule's

LUMO). This suggests that atom 18 is interacting with an electron- deficient center. The case of negative values for S^N_{18}(LUMO)* leads to a similar conclusion (for a detailed discussion of positive and negative values of S^N (see [28]). Note that $(LUMO)_{18}$* has a π nature in all molecules (Table 7). This suggests that possible interactions could be of π-π stacked, π-π T-shaped or π-cation kinds. Atom 16 is a nitrogen of the chain linking rings C and D (Fig. 2). If S^N_{16}(LUMO)* values are positive, a good percentage of inhibition is associated with high numerical values for this index. This, in turn, indicates that a high reactive (LUMO)* is needed. This suggests that atom 16 is interacting with an electron-rich center. All the aforementioned ideas are depicted in the partial two dimensional (2D) pharmacophore shown in Fig. 5.

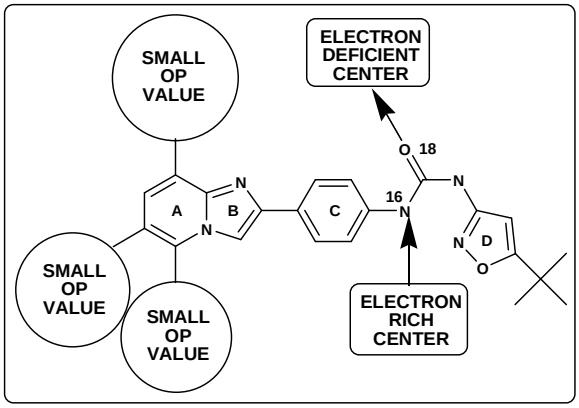

Figure 5. Partial 2D pharmacophore for the percentage of inhibition of FLT3

Discussion of the inhibition of MV4-11 cells.

Before discussing our results, it must be noted that the mechanism or mechanisms of the antiproliferative activity are not known. As we noted earlier [12] the fact that statistically significant results are obtained is a good indication that all molecules go through the same step or steps to exert their effect. The beta values (Table 4) show that the importance of variables is φ_{R1}> S^N_{18}(LUMO)*> S^E_8(HOMO-2)*> S^N_{28}(LUMO)*> F_{13}(LUMO+1)*>> S^N_6(LUMO)*. A good inhibitory activity is associated with low numerical values for log(IC_{50}). For the orientational parameter φ_{R1}, and employing the same abovementioned analysis, we conclude that a high antiproliferative activity is associated with small numerical values for this index. Atom 28 is a carbon of the tert-butyl substituent in ring D (Fig. 2). A high antiproliferative activity is associated with high values of S^N_{28}(LUMO)* if the numerical values of this index are positive. This suggests that atom 28 is interacting with an electron-rich center. Given that $(LUMO)_{28}$* has a σ nature in all molecules (Table 7), we tentatively suggest that this atom could be engaged in C-H or weak σ-π interactions with residues forming an hydrophobic region. Atom 18 is the carbonyl oxygen of the chain linking ring D and E (Fig. 2). A high antiproliferative activity is associated with high values of S^N_{18}(LUMO)* if the numerical values for this index are negative. Higher negative values are obtained by shifting upwards the energy of corresponding eigenvalue making the MO more reactive. Therefore we suggest that atom 18 is interacting with an electron-rich center. $(LUMO)_{18}$* has a π nature in all molecules (Table 7). Possible interactions are π-anion, π-π stacked or π-π T-shaped. A hydrogen bond should not be discarded. Atom 13 is a carbon in ring B (Fig. 2). A high antiproliferative activity is associated with high values of F_{13}(LUMO+1)*. $(LUMO)_{13}$* and $(LUMO+1)_{13}$* have a π nature in all molecules (Table 6). This suggests that atom 13 is interacting with an electron-rich center through its two lowest vacant MOs. Atom 8 is a carbon in ring B (Fig. 2). A high antiproliferative activity is associated with low (negative) numerical values of S^E_8(HOMO-2)*. Table 8 shows that the three highest occupied local MOs have a π nature. A graphical analysis of log(IC_{50}) *versus* S^E_8(HOMO-1)* and S^E_8(HOMO)* shows that a high antiproliferative activity is associated with low (negative) numerical values of S^E_8(HOMO-1)* and with high (negative) values of S^E_8(HOMO)*. Both variables do not appear in the regression equation because the variation of their values is not statistically significant. As we said in other papers, the use of statistical analysis instead of solving the linear system of equations is the weak point of this method (see [9]). Now, to get low (negative) numerical values for S^E_8(HOMO-1)* and S^E_8(HOMO-2)*, we need to shift downwards the energy of the corresponding eigenvalues. An additional possibility is finding a substitution removing the localization of the MOs on atom 8. Therefore, it seems that atom 8 is interacting with an electron-deficient center through its highest occupied local MO. The antiproliferative activity may be improved by making $(HOMO)_8$* more reactive. Atom 6 is a carbon in

ring A (Fig. 2). A high antiproliferative activity is associated with high values of S^N_6(LUMO)* if the numerical values of this index are positive. Therefore, atom 6 seems to interact with an electron-rich center through its lowest vacant MO. All the above-mentioned ideas are depicted in the partial two dimensional (2D) pharmacophore shown in Fig. 6.

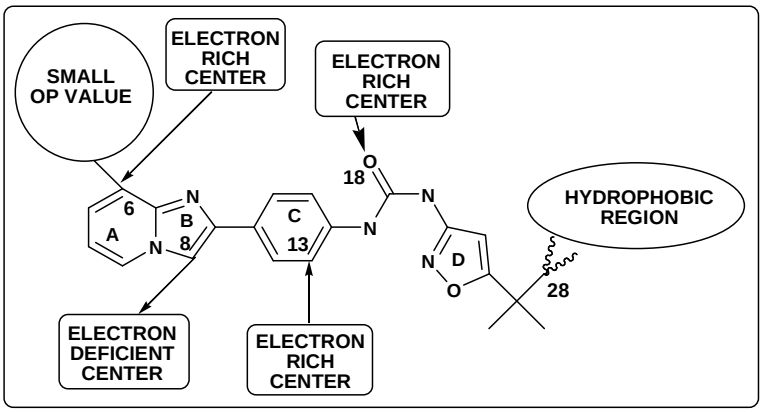

Figure 6. Partial 2D pharmacophore for the inhibition of MV4-11 cells

Note that the two biological processes seem to be orbital- and sterically-controlled.

In conclusion, we have obtained statistically significant equations for both biological activities. This paper shows the advantages of using Quantum Chemistry as a tool for drug design.

REFERENCES

[1] M. Andreeff, *Targeted therapy of acute myeloid leukemia*, Springer Verlag, Heidelberg, **2015**.
[2] D. Sun, Y. Yang, J. Lyu, W. Zhou, W. Song, Z. Zhao, Z. Chen, Y. Xu, H. Li, *J. Med. Chem.*, **2016,** 59, 6187-6200.
[3] B. Mashkani, M. H. Tanipour, M. Saadatmandzadeh, L. K. Ashman, R. Griffith, *Eur. J. Pharmacol.*, **2016,** 776, 156-166.
[4] Y. Xu, N.-Y. Wang, X.-J. Song, Q. Lei, T.-H. Ye, X.-Y. You, W.-Q. Zuo, Y. Xia, L.-D. Zhang, L.-T. Yu, *Bioorg. Med. Chem.*, **2015,** 23, 4333-4343.
[5] G. Liu, S. Abraham, X. Liu, S. Xu, A. M. Rooks, R. Nepomuceno, A. Dao, D. Brigham, D. Gitnick, D. E. Insko, M. F. Gardner, P. P. Zarrinkar, R. Christopher, B. Belli, R. C. Armstrong, M. W. Holladay, *Bioog. Med. Chem. Lett.*, **2015,** 25, 3436-3441.
[6] J. T. A. Hsu, T.-K. Yeh, S.-C. Yen, C.-T. Chen, S.-Y. Hsieh, T. Hsu, C.-T. Lu, C.-H. Chen, L.-H. Chou, C.-H. Chiu, Y.-I. Chang, Y.-J. Tseng, K.-R. Yen, Y.-S. Chao, W.-H. Lin, W.-T. Jiaang, *Bioog. Med. Chem. Lett.*, **2012,** 22, 4654-4659.
[7] J. J. Chen, K. D. Thakur, M. P. Clark, S. K. Laughlin, K. M. George, R. G. Bookland, J. R. Davis, E. J. Cabrera, V. Easwaran, B. De, Y. George Zhang, *Bioog. Med. Chem. Lett.*, **2006,** 16, 5633-5638.
[8] J. S. Gómez Jeria, *Boll. Chim. Farmac.*, **1982,** 121, 619-625.
[9] J. S. Gómez-Jeria, *Int. J. Quant. Chem.*, **1983,** 23, 1969-1972.
[10] J. S. Gómez-Jeria, "Modeling the Drug-Receptor Interaction in Quantum Pharmacology," in *Molecules in Physics, Chemistry, and Biology*, J. Maruani Ed., vol. 4, pp. 215-231, Springer Netherlands, 1989.
[11] J. S. Gómez-Jeria, M. Ojeda-Vergara, *J. Chil. Chem. Soc.*, **2003,** 48, 119-124.
[12] J. S. Gómez-Jeria, M. Flores-Catalán, *Canad. Chem. Trans.*, **2013,** 1, 215-237.
[13] J. S. Gómez-Jeria, *Res. J. Pharmac. Biol. Chem. Sci.*, **2016,** 7, 288-294.
[14] J. S. Gómez-Jeria, *Res. J. Pharmac. Biol. Chem. Sci.*, **2016,** 7, 2258-2260.
[15] J. S. Gómez-Jeria, D. Morales-Lagos, "The mode of binding of phenylalkylamines to the Serotonergic Receptor," in *QSAR in design of Bioactive Drugs*, M. Kuchar Ed., pp. 145-173, Prous, J.R., Barcelona, Spain, 1984.
[16] J. S. Gómez-Jeria, D. R. Morales-Lagos, *J. Pharm. Sci.*, **1984,** 73, 1725-1728.
[17] J. S. Gómez-Jeria, B. K. Cassels, J. C. Saavedra-Aguilar, *Eur. J. Med. Chem.*, **1987,** 22, 433-437.

[18] J. S. Gómez-Jeria, M. Ojeda-Vergara, C. Donoso-Espinoza, *Mol. Engn.*, **1995,** 5, 391-401.
[19] J. S. Gómez-Jeria, L. Lagos-Arancibia, E. Sobarzo-Sánchez, *Bol. Soc. Chil. Quím.*, **2003,** 48, 61-66.
[20] J. S. Gómez-Jeria, L. A. Gerli-Candia, S. M. Hurtado, *J. Chil. Chem. Soc.*, **2004,** 49, 307-312.
[21] J. S. Gómez-Jeria, F. Soto-Morales, J. Rivas, A. Sotomayor, *J. Chil. Chem. Soc.*, **2008,** 53, 1393-1399.
[22] J. S. Gómez-Jeria, *Int. Res. J. Pure App. Chem.*, **2014,** 4, 270-291.
[23] J. S. Gómez-Jeria, *Brit. Microbiol. Res. J.*, **2014,** 4, 968-987.
[24] J. S. Gómez-Jeria, *SOP Trans. Phys. Chem.*, **2014,** 1, 10-28.
[25] J. S. Gómez-Jeria, *Res. J. Pharmac. Biol. Chem. Sci.*, **2014,** 5, 424-436.
[26] J. S. Gómez-Jeria, *Res. J. Pharmac. Biol. Chem. Sci.*, **2015,** 6, 688-697.
[27] J. S. Gómez-Jeria, V. Gazzano, *Der Pharma Chem.*, **2016,** 8, 21-27.
[28] J. S. Gómez-Jeria, M. Matus-Perez, *Der Pharma Chem.*, **2016,** 8, 1-11.
[29] J. S. Gómez-Jeria, C. Moreno-Rojas, *Der Pharma Chem.*, **2016,** 8, 475-482.
[30] J. S. Gómez-Jeria, Í. Orellana, *Der Pharma Chem.*, **2016,** 8, 476-487.
[31] J. S. Gómez-Jeria, *Canad. Chem. Trans.*, **2013,** 1, 25-55.
[32] J. S. Gómez-Jeria, *Elements of Molecular Electronic Pharmacology (in Spanish),* Ediciones Sokar, Santiago de Chile, **2013**.
[33] M. J. Frisch, G. W. Trucks, H. B. Schlegel, G. E. Scuseria, M. A. Robb, J. R. Cheeseman, J. Montgomery, J.A., T. Vreven, K. N. Kudin, J. C. Burant, J. M. Millam, S. S. Iyengar, J. Tomasi, V. Barone, B. Mennucci, M. Cossi, G. Scalmani, N. Rega, G03 Rev. E.01, Gaussian, Pittsburgh, PA, USA, **2007**.
[34] J. S. Gómez-Jeria, D-Cent-QSAR: A program to generate Local Atomic Reactivity Indices from Gaussian 03 log files. v. 1.0, Santiago, Chile, **2014**.
[35] J. S. Gómez-Jeria, *J. Chil. Chem. Soc.*, **2009,** 54, 482-485.
[36] Statsoft, Statistica v. 8.0, 2300 East 14 th St. Tulsa, OK 74104, USA, 1984-**2007**.